A Multiwall Carbon Nanotubes Paste Electrode as a Sensor and Ferrocenemonocarboxylic Acid as a Mediator for Electrocatalytic Determination of Isoproterenol

Ali A. Ensafi[*], Hassan Karimi Maleh

Department of Chemistry, Isfahan University of Technology, Isfahan 84156–83111, Iran
[*]E–mail: ensafi@cc.iut.ac.ir

A ferrocenemonocarboxylic acid modified carbon nanotubes paste electrode (FMAMCNTPE) was constructed and used as a fast and sensitive tool for the determination of isoproterenol (ISPT) at trace level. It has been shown by direct current cyclic voltammetry, double step chronoamperometry and electrochemical impedance spectroscopy (EIS) that this modified electrode can catalyze the oxidation of ISPT in aqueous solution. The kinetic parameters of the system including electron transfer coefficient, and rate constant for the chemical reaction between ISPT and the redox sites in FMAMCNTPE were also determined using the electrochemical approaches. In addition, differential pulse voltammetry (DPV) was used for quantitative analysis. DPV showed wide linear dynamic range $(0.5 - 50.0 \ \mu mol \ L^{-1} \ ISPT)$ with a detection limit of $0.2 \ \mu mol \ L^{-1} \ ISPT$. The relative standard deviation (*RSD%*) for ten successive assays of $5.0 \ \mu mol \ L^{-1} \ ISPT$ was 1.9%. Finally, this method was also examined as a selective, simple and precise electrochemical sensor for the determination of ISPT in real samples such as drug and urine.

1. INTRODUCTION

Isoproterenol or isoprenaline (4-[1-hydroxy-2-[(1-methylethyl)-amino] ethyl]-1,2-benzenediol) is a ß-adrenergic stimulant which has been used for the treatment of primary pulmonary hypertension and also has been employed as an adrenergic acceptor, contributing to the research of other bronchodilators as terbutaline, fenoterol, salbutamol and others [1]. It is one of catecholamine compound that consists of an amine attached to a benzene ring bearing two hydroxyl groups (catechol) [2]. The cardiovascular effects of isoprenaline compare with epinephrine and norepinephrine, which

can relax almost every kind of smooth musculature that contains adrenergic nerves, but this effect is pronounced in the musculature of bronchus and also in the gastrointestinal tract [3]. ISPT has positive inotropic and chronotropic effects on the heart. Various methods including gas chromatography [4], chemiluminescence (CL) [5–7], spectrophotometric [8–12] and electrochemical method [13] have been used for the detection of ISPT.

Nanotechnology has become one of the most interesting disciplines in science and technology today. The intense interest in nanotechnology is being driven by various interesting fields and is leading to a new industrial revolution. Carbon nanotubes (CNT) are an important nano structural that used building blocks of nanotechnology. With one hundred times the tensile strength of steel, thermal conductivity better than all but the purest diamond, and electrical conductivity similar to copper, but with the ability to carry much higher currents, they seem to be a very interesting material. Since their discovery in 1991 [14], CNTs have generated great interest for future applications based on their field emission and electronic transport properties [15], their high mechanical strength [16] and high conductivity [17,18]. The modification of electrode substrates with CNTs for use in analytical sensing has been documented to result in low detection limits, high sensitivities, reduction of over-potentials, and resistance to surface fouling [19–24].

In this study, we used voltammetric and electrochemical impedance spectroscopic techniques at pH 5.0 to demonstrate the electrochemical behavior of ISPT on a multiwall carbon nanotubes paste electrode modified with ferrocenemonocarboxylic acid as a mediator. The proposed method has been used in the determination of ISPT in pharmaceutical and urine samples.

2. EXPERIMENTAL

2.1. Chemicals

All chemicals used were of analytical reagent grade purchased from Merck (Darmstadt, Germany) unless otherwise stated. Doubly distilled water was used throughout. Ferrocenemonocarboxylic acid was used from Fluka and ISPT from Aldrich, all used as received.

A 1.0×10^{-2} mol L^{-1} ISPT solution was prepared daily by dissolving 0.062 g isoproterenol in water and the solution was diluted to 25 mL with water in a 25−mL volumetric flask. The solution was kept in the refrigerator at 4 ^{o}C in the dark. More dilute solutions were prepared by serial dilution with water.

Phosphate buffer (sodium dihydrogen phosphate and disodum monohydrogen phophate plus sodium hydroxide, 0.1 mol L^{-1}) solutions (PBS) with different pH values were used.

Spectrally pure graphite powder (particle size<50 μm) from Merck, high viscose paraffin oil (density = 0.88 Kg L^1) from Merck, and multiwall carbon nanotube (>90% MWCNT basis, d × 1 = (110 − 70 nm) × (5 − 9 μm) from Fluka were used for the preparation of the carbon paste electrode (CPE).

2.2. Apparatus

Cyclic voltammetry (CV) and differential pulse voltammetry (DPV) were performed in an analytical system, Micro-Autolab, potentiostat/galvanostat connected to a three electrode cell, Metrohm Model 663 VA stand, linked with a computer (Pentium IV, 1200 MHz) and with micro-Autolab software. In addition, impedance spectroscopy was performed in an analytical system, Autolab PGSTAT 12, potentiostat/galvanostat connected to a three-electrode cell, Metrohm Model 663 VA stand, linked with a computer (Pentium IV, 1200 MHz) and with Autolab software. The system was run on a PC using GPES and FRA 4.9 software. For impedance measurements, a frequency range of 100 kHz to 1.0 Hz was employed. The AC voltage amplitude used was 5 mV, and the equilibrium time was 10 minutes. A conventional three-electrode cell assembly consisting of a platinum wire as an auxiliary electrode and an Ag/AgCl (KCl$_{sat}$) electrode as a reference electrode was used. The working electrode was either an unmodified carbon nanotube paste electrode (CNPE) or a carbon nanotubes paste electrode modified with ferrocenemonocarboxylic acid (FMAMCNTPE). The prepared electrodes with carbon nanotubes and with the modifier were characterized by scanning electron microscopy (SEM) (XLC Philips).

A pH–meter (Corning, Model 140) with a double junction glass electrode was used to check the pH of the solutions.

2.3. Preparation of the electrode

3.0 mg ferrocenemonocarboxylic acid hand mixed with 87.0 mg of graphite powder and 10.0 mg of multiwall carbon nanotubes in a mortar and pestle. Using a syringe, 0.50 g of paraffin was added to the mixture and mixed well for 40 min until a uniformly-wetted paste was obtained. The paste was then packed into a glass tube. Electrical contact was made by pushing a copper wire down the glass tube into the back of the mixture. When necessary, a new surface was obtained by pushing an excess of the paste out of the tube and polishing it on a weighing paper. The unmodified carbon paste electrode (CPE) was prepared in the same way without adding ferrocene and carbon nanotubes to the mixture to be used for comparison purposes.

2.4. Preparation of real ramples

Ampoule (0.2 mg/mL) prepared and then 0.1 mL of the solution plus 10 mL of 0.1 mol L^{-1} buffer (pH 5.0) was used for the analysis.

The urine samples were stored in a refrigerator immediately after collection. Ten milliliters of the sample was centrifuged for 10 min at 2000 rpm. The supernatant was filtered using a 0.45 µm filter and then diluted 5–times with universal buffer pH 5.0. The solution was transferred into the voltammetric cell to be analyzed without any further pretreatment. Standard addition method used for the determination of ISPT in real samples.

2.5. Recommended procedure

The modified multiwall carbon nanotubes paste electrode was polished with a white clean paper. To prepare a blank solution, 10.0 mL of buffer solution (PBS, pH 5.0) was transferred into an electrochemical cell. The initial and final potentials were adjusted to +0.20 and +0.80 V *vs*. Ag/AgCl, respectively. DPV was recorded with pulse height and pulse width of 50 mV and 0.5 mV to give the blank signal and labeled as I_{pb}. Then, different amounts of ISPT were added to the cell, using a micropipette, and the DPV was recorded again to get the analytical signal (I_{ps}). Calibration curves were constructed by plotting the net catalytic peak current (ΔI_p) *vs*. the ISPT concentration.

3. RESULTS AND DISCUSSION

3.1. SEM Characterization

Figure 1 displays a typical morphology of the modified multiwall carbon nanotubes paste electrode with ferrocenemonocarboxylic acid (a), and with an unmodified carbon paste electrode (b) characterized by SEM.
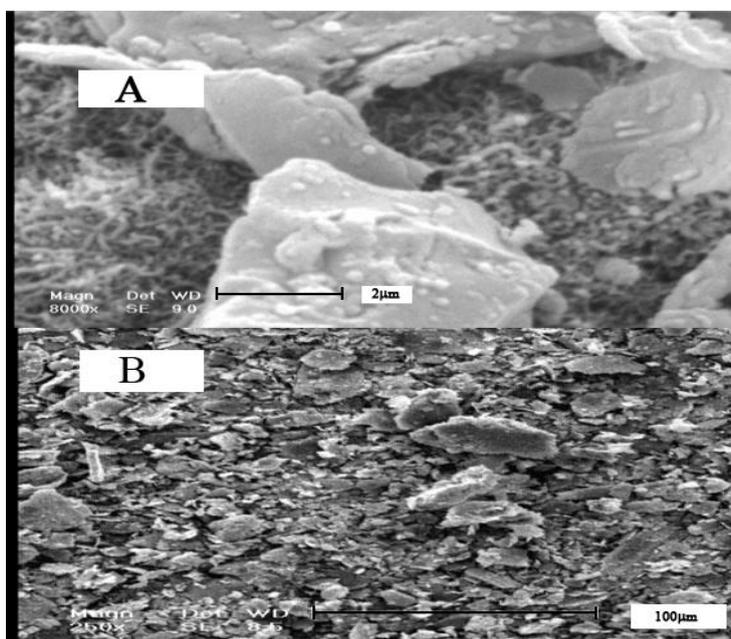
Figure 1. SEM image of: (A) FMAMCNTPE and (B) CNPE.

As shown in Fig. 1, ferrocenedicarboxylic acid on the surface of CNTs did not change the morphology of CNTs, but made it more compact. However, it can be clearly seen that MWCNTs dispersed homogeneously.

3.2. Electrochemistry of the mediator

The cyclic voltammogram results showed a well-defined and reproducible anodic and cathodic peaks related to Fc/Fc$^+$ redox couple with quasi-reversible behavior, with peak separation potential of ΔEp ($E_{pa} - E_{pc} = 100$ mV) (Fig. 2).
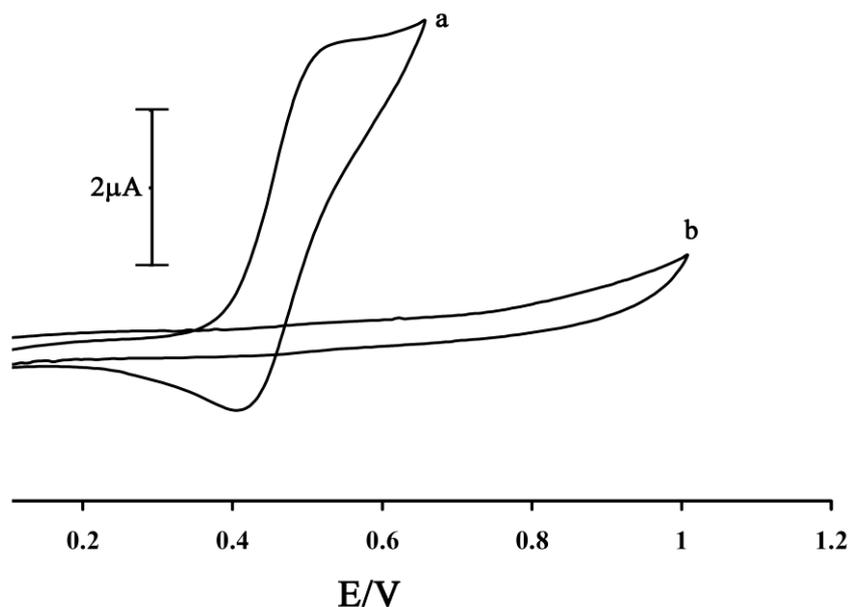
Figure 2. The cyclic voltammograms of a) FMAMCNTPE and b) bare CPE in 0.1 mol L^{-1} phosphate buffer solution (pH 5.0) at a scan rate 20 mV s^{-1}.
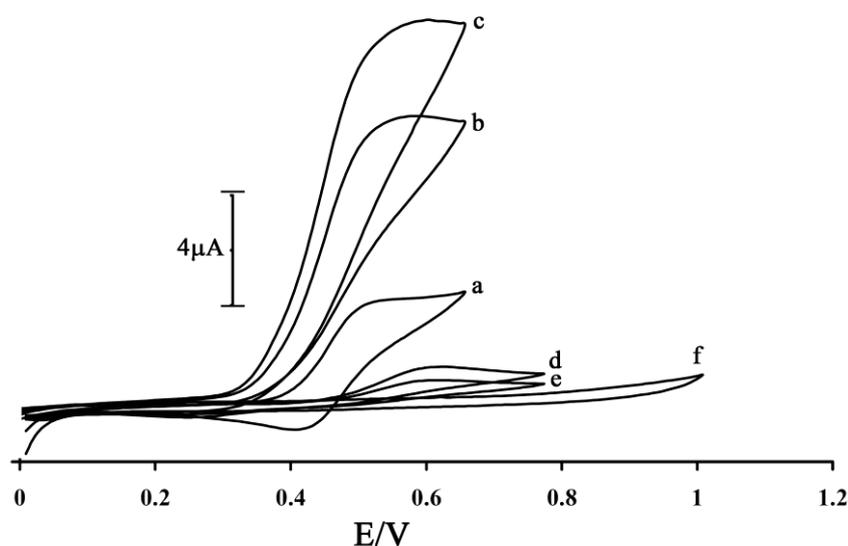
Figure 3. Cyclic voltammograms of 0.1 mol L^{-1} buffer solution (pH 5.0) with a scan rate of 20 mV s^{-1} for: (a) in the absence and (b): in the presence of 200 μmol L^{-1} ISPT at FMAMCPE respectively. (c) is as (b) at FMAMCNTPE. (d) is as (c) and (e) is as (b) at CNPE and at CPE, respectively. (f) is as (a) without mediator.

These cyclic voltammograms were used to examine the variation of the peak currents *vs.* the potential scan rates. The plots of the anodic and cathodic peak currents were linearly dependent on $\upsilon^{1/2}$ at the all scan rates. This behavior indicates that the nature of redox process is diffusion controlled [19].

The cyclic voltammetric results of the modified electrode in various buffered solutions did not show any shift in the anodic and cathodic peak potentials. Therefore, the electrochemical behavior of the redox process of Fc/Fc^+ in FMAMCNTPE is independent to pH of the solution.

3.3. Catalytic effect

Figure 3(b–e) shows the cyclic voltammetric responses from electrochemical oxidation of 200 μmol L^{-1} ISPT at different electrodes including FMAMCNTPE (curve c), ferrocenemonocarboxylic acid-modified carbon paste electrode (FMAMCPE) (curve b), carbon nanotubes paste electrode (CNTPE) (curve d), and carbon paste electrode (curve e). However, curve f shows cyclic voltammogram carbon paste electrode in the buffer solution (pH 5.0). The anodic peak potential for ISPT oxidation at FMAMCNTPE (curve c) and at FMAMCPE (curve b) was about 520 mV, while at CNTPE (curve d) was about 600 mV. The peak potential of ISPT was about 610 mV (curve e) at the unmodified carbon paste electrode (CPE). Based on these results, the best electrocatalytic effect for ISPT oxidation was found at FMAMCNTPE (curve c). The peak potential of ISPT oxidation at FMAMCNTPE (curve c) was shifted by about 80 and 90 mV toward negative values in compared with that at CNTPE (curve d) and at CPE (curve e), respectively.

Similarly, the anodic peak current for the oxidation of ISPT at FMAMCNTPE (curve c) was significantly enhanced in comparison to that at FMAMCPE (curve b). The data clearly shows that the combination of multiwall carbon nanotubes and the mediator definitely improves the characteristics of ISPT oxidation. FMAMCNTPE in 0.1 mol L^{-1} phosphate buffer (pH 5.0) and without ISPT in solution exhibited a well-behaved redox reaction (curve a).
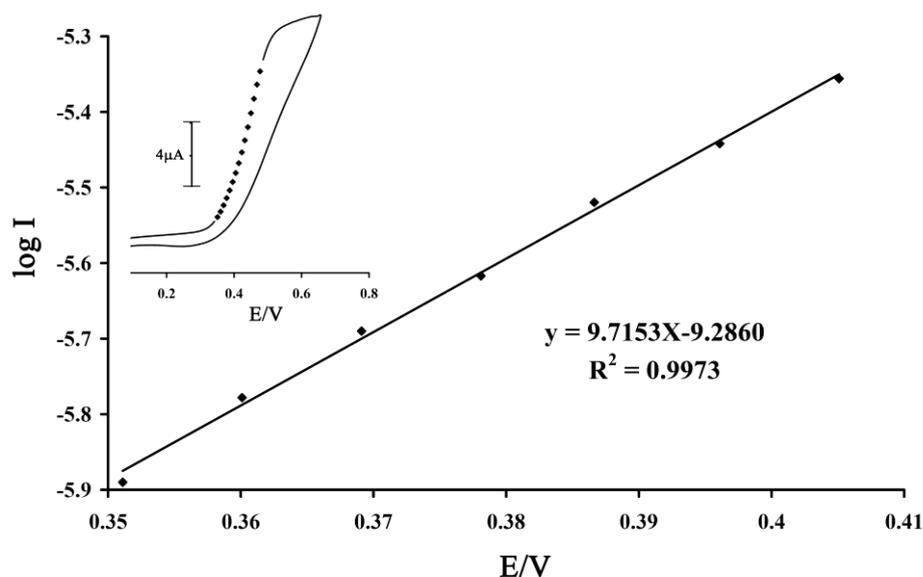
Figure 4. Tafel plot for FMAMCNTPE in 0.1 mol L^{-1} PBS (pH 5.0) with a scan rate of 18 mV s^{-1} in the presence of 20.0 μmol L^{-1} ISPT.

In order to obtain information on the rate determining step, a Tafel plot was developed for FMAMCNTPE, using the data derived from the raising part of the current–voltage curve (Fig. 4, inset A). The slope of the Tafel plot is equal to $n(1-\alpha)F/2.3RT$ which comes up to 9.715 V decade^{-1}. Assuming n = 2, then α = 0.71.

In addition, the value of αn_α (n_α is the number of electrons involved in the rate determining step) was calculated for the oxidation of ISPT at pH 5.0 for both the modified and unmodified carbon nanotube paste electrodes using the following equation [25-27]:

$$\alpha n_\alpha = 0.048/(E_P - E_{P/2}) \qquad (1)$$

where $E_{P/2}$ is the potential corresponding to $I_{P/2}$. The values for αn_α were found to be 0.70 and 0.23 at the surface of both FMAMCNTPE and the unmodified carbon nanotube paste electrode, respectively. These values showed that the over-potential of ISPT oxidation is reduced at the surface of FMAMCNTPE, and also that the rate of electron transfer process is greatly enhanced. This phenomenon is, thus, confirmed by the larger I_{pa} values recorded during cyclic voltammetry at FMAMCNTPE.
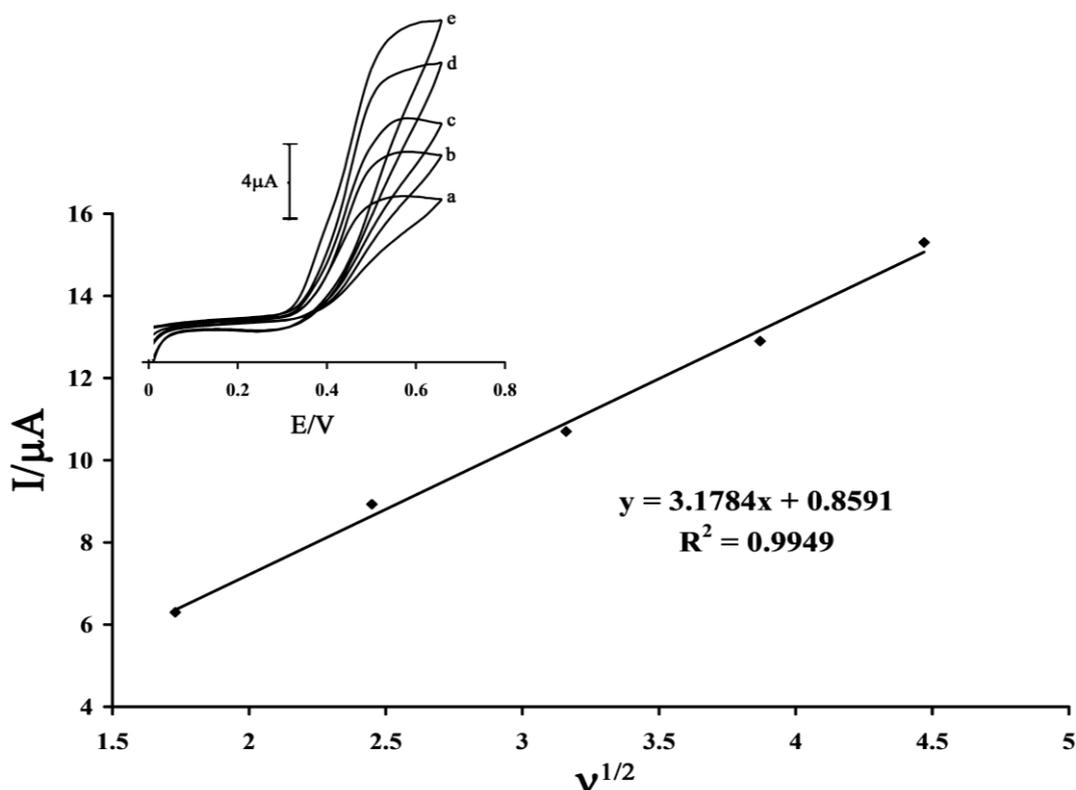
Figure 5. Plot of I_{pa} versus $v^{1/2}$ for the oxidation of ISPT at FMAMCNTPE. Insert A) Cyclic voltammograms of 180 µmol L^{-1} ISPT at various scan rates; 1) 2.0; 2) 6.0; 3) 10.0; 4) 15 and 5) 20 mV s^{-1} in 0.1 mol L^{-1} PBS (pH 5.0).

Also, a plot of peak height (I_p) versus the square root of the scan rate ($v^{1/2}$), over the range of 3 – 20 mV s^{-1}, was constructed. This plot was found to be linear, suggesting that the process (at sufficient overpotential) was diffusion rather than surface controlled (Fig. 5).

3.4. Chronoamperometric study

Double step potential chronoamperometry was employed for investigation the electrochemical processes of FMAMCNTPE (Fig. 6).
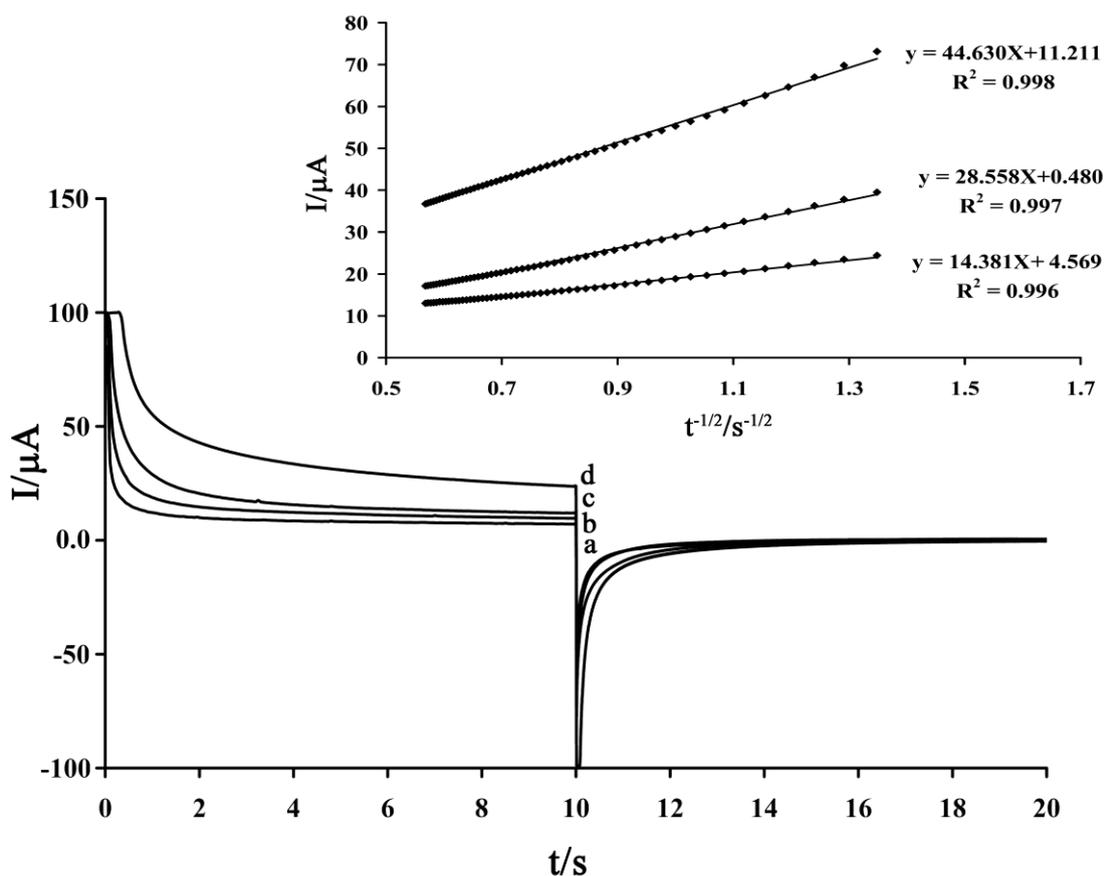
Figure 6. Chronoamperograms obtained at FMAMCNTPE a) in the absence, and in the presence of b) 200, c) 300 and d) 500 μmol L^{-1} ISPT at pH 5.0.

In chronoamperometric studies, we have determined the diffusion coefficient, D, of ISPT. The experimental plots of I versus t$^{-1/2}$ with the best fits for different concentrations of ISPT were employed (Fig. 6, inset). The slopes of the resulting straight lines were then plotted versus the ISPT concentrations, from whose slope and using the Cottrell equation [28]:

$$I = nFAD^{1/2}C_b\pi^{-1/2}t^{-1/2} \qquad (1)$$

We calculated a diffusion coefficient as 7.4×10^{-5} cm^2 s^{-1} for ISPT.

The rate constant for the chemical reaction between ISPT and redox sites in FMAMCNTPE, k_h, can be evaluated by chronoamperometry according to the method of Galus [29]:

$$I_C/I_L = \pi^{1/2}(kC_bt)^{1/2} \qquad (2)$$

Based on the slope of the I_C/I_L versus $t^{1/2}$ plots, we calculate k_h as 4.85×10^3 M^{-1} s^{-1}.

3.5. Electrochemical impedance spectroscopy study

Electrochemical impedance spectroscopy (EIS) was also employed to investigate the oxidation of ISPT at FMAMCNTPE (Fig. 7).
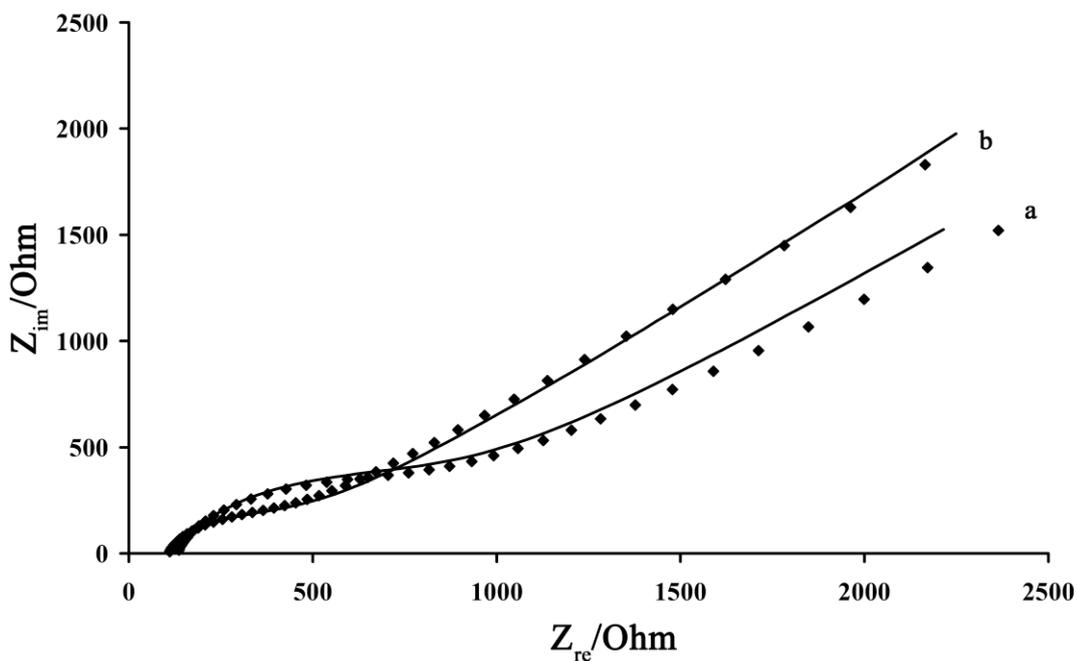
Figure 7. Nyquist diagrams of FMAMCNTPE in the absence (a) and presence of (b) 500.0 μmol L^{-1} ISPT at pH 5.0. Bias is 0.40 V with *Eac* = 5 mV with frequency range of 10 kHz to 0.1 Hz.

The electrical equivalent circuit (from modified electrode in the absence and presence of ISPT) compatible with the impedance spectra are shown in scheme 1, which incorporates R_s (thesolution/electrolyte resistance), R_{ct} (charge-transfer resistance), Z_w (Warburg impedance) related to the semi-infinite linear diffusion, and Q (constant phase element).
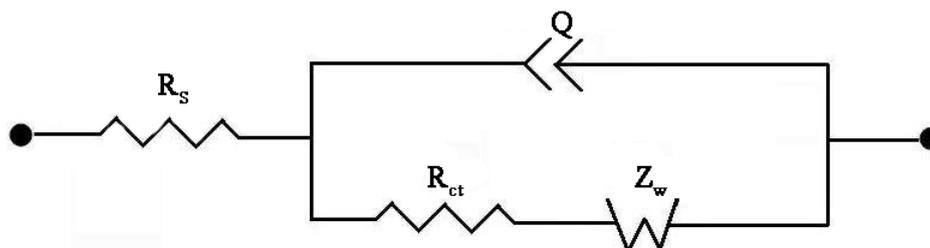
Scheme 1. Equivalent circuit for the system

The appearance of both kinetic (R_{ct}) and diffusion (Z_w) domains indicates mixed electrode reactions. In the presence of ISPT, the diameter of the semicircle decreases, confirming the electrocatalytic capability of the mentioned electrocatalyst for the oxidation of ISPT. This is due to the instant chemical reaction of ISPT with the high-valence of ferrocenemonocarboxylic acid species. The catalytic reaction of the oxidation of ISPT that occurred via the participation of ferrocenemonocarboxylic acid species virtually caused an increase in the surface concentration of low valence species of electrocatalyst, and the charge-transfer resistance declined, depending on the concentration of ISPT in the solution.

3.6. Stability and reproducibility

The repeatability and stability of FMAMCNTPE was investigated using cyclic voltammogram of 5.0 μmol L^{-1} ISPT. The relative standard deviation (*RSD%*) for ten successive assays was 1.9%. When used five different electrodes, the *RSD%* for five measurements was 2.3%. When the modified electrode stored in the libratory, the modified electrode retains 96% of its initial response after 7 days and 92% after 40 days. These results indicate that FMAMCNTPE has a good stability and reproducibility, and could be used for ISPT.

4. DYNAMIC RANGE AND DETECTION LIMIT

Differential pulse voltammetry (DPV) was used to determine the concentration of ISPT in solution. The results showed two linear segments with different slopes for ISPT concentration; namely, for 0.5 – 3.1 μmol L^{-1} of ISPT, the regression equation was $\Delta I_p(\mu A) = 2.1045 C_{ISPT} + 0.1835$ ($r^2 = 0.9931$, n = 5), while for 3.1 – 50.0 μmol L^{-1} of ISPT, the regression equation was $\Delta I_p(\mu A) = 0.6754 C_{ISPT} + 3.9962$ ($r^2 = 0.9917$, n = 7), where C_{ISPT} is μmol L^{-1} concentration of ISPT. The detection limit was determined at 0.2 μmol L^{-1} ISPT according to the definition of $Y_{LOD} = Y_B + 3\sigma$ [30].

5. INTERFERENCE STUDY

The influence of various substances as potential interfering compounds with the determination of ISPT was studied under the optimum conditions with 5.0 µmol L^{-1} ISPT at pH 5.0. The potentially interfering substances were chosen from the group of substances commonly found with ISPT in pharmaceuticals and/or in biological fluids. The tolerance limit was defined as the maximum concentration of the interfering substance that caused an error of less than ±5% for the determination of ISPT. After the experiments, we found that neither 800–fold of glucose, sucrose, lactose, fructose nor 600–fold of Ca^{2+}, Mg^{2+}, SO_4^{2-}, Al^{3+}, NH_4^+, Br^-, and F^- affected the selectivity. Nor did saturation of starch solution and 300–fold of urea and thiourea interfere with the determination of ISPT.

6. REAL SAMPLE DETERMINATION

In order to evaluate the applicability of the proposed method for the determination of isoproterenol in real samples, its utility was tested by determining isoproterenol in ampoule and in urine samples. The results are given in Table 1. The results indicate that the determination of isoproterenol using the electrode is effective and can be applied for their detection of isoproterenol in real samples.

Table 1. Determination of ISPT in drug and urine samples.

Sample	Added (µmol L^{-1})	Expected (µmol L^{-1})	Founded (µmol L^{-1})	RSD(%)
1 Urine	——	——	<detection limit	——
2	3.00	3.00	3.08 ± 0.05	2.1
3	2.00	5.00	5.15 ± 0.06	2.3
4 Ampoule	——	5.00	4.85 ± 0.04	1.9
5	5.00	10.00	9.92 ± 0.07	2.5

Average of five replicate measurements.

7. CONCLUSION

This work describes the ability of the modified multiwall carbon nanotubes paste electrode for catalytic determination of ISPT. The results demonstrated that the electrooxidation of ISPT at the surface FMAMCNTPE occurs at potential about 80 mV less positive that at a bare carbon paste electrode. The kinetic parameter of the electrocatalytic process, the diffusion coefficients of ISPT in an aqueous solution was determined. Finally, this method was also examined as a selective, simple and precise electrochemical sensor for the determination of ISPT in real samples such as drug and urine.

References

1. The Merck Index, Merck & Co., 1996, p. 890.
2. L.S. Goodman, A. Gilman, The Pharmacological Basis of Therapeutics, 9th ed., McGraw-Hill, New York, 1996**,** pp. 105–109.
3. V.G. Bonifácio, L.H. Marcolino Jr., M.F.S. Teixeira, O. Fatibello-Filho, *Microchem. J.* 78 (2004) 55.
4. J.R. Watson, R.C. Lawrence, *J. Pharm. Sci.* 66 (1977) 560.
5. G.J. Zhou, G.F. Zhang, H.Y. Chem, *Anal. Chim. Acta,* 463 (2002) 257.
6. C. Zhang, J. Huang, Z. Zhang, M. Aizawa, *Anal. Chim. Acta,* 374 (1998) 105.
7. A.A. Al-Warthan, S.A. Al-Tamrah, A. Al-Akel, *Anal. Sci.* 10 (1994) 449.
8. K.O. Lupetti, I.C. Vieira, O. Fatibello-Filho, *Talanta,* 57 (2002) 135.
9. P. Solich, Ch.K. Polydorou, M.A. Koupparis, C.E. Efstathiou, *J. Pharm. Biomed. Anal.* 22 (2000) 781.
10. J.J.B. Nevado, J.M.L. Gallego, P.B. Laguna, *Anal. Chim. Acta,* 300 (1995) 293–297.
11. H.A. El-Obeid, *Anal. Lett.* 17 (1984) 771.
12. R.M.V. Camanˇas, J.M.S. Mallols, J.R.T Lapasio´, G. Ramis-Ramos, *Analyst,* 120 (1995) 1767.
13. A.Kutluay, M. Aslanoglu, *Acta Chim. Slov.* 57 (2010) 157.
14. S. Iijima, *Nature,* 354 (1991) 56.
15. W.Z.Li, S.S. Xie, L.X. Qian, B.H. Chang, B.S. Zou, W.Y. Zhou, R.A. Zhao, G. Wang, *Science,* 274 (1996*)* 1701.
16. M.M. Treachy, T.W. Ebbesen, J.M. Gibson, *Nature,* 381 (1996) 678.
17. A.A. Ensafi, H. Karimi-Maleh, *J. Electroanal. Chem.* 640 (2010) 75.
18. H. Beitollahi, H. Karimi-Maleh, H. Khabazzadeh, *Anal. Chem.* 80 (2008) 9848.
19. A.A. Ensafi, M. Taei, and T. Khayamian, *Int. J. Electrochem. Sci.* 5 (2010) 116.
20. A.A. Ensafi, B. Rezaei, E. Khoddami, H. Karimi-Maleh, *Colloid & Surfaces B,* 81 (2010) 42.
21. P. Norouzi, F. Faridbod, B. Larijani, M.R. Ganjali, *Int. J. Electrochem. Sci.* 5 (2010) 1213.
22. M. Mazloum-Ardakani, H. Beitollahi, B. Ganjipour, H. Naeimi, *Int. J. Electrochem. Sci.* 5 (2010) 531.
23. A.A. Ensafi, H. Karimi-Maleh, *Electroanalysis*, DOI: 10.1002/elan.201000270, in press.
24. A.A. Ensafi, M. Taei, T. Khayamian, F. Hasanpour, *Anal. Sci.* 26 (2010) 803.
25. M.H. Pournaghi-Azar, H. Razmi-Nerbin, *J. Electroanal. Chem.* 488 (2000) 17.
26. J.B. Raoof, R. Ojani, H. Karimi-Maleh, *Electroanalysis,* 2008, *20,* 129–1262.
27. A.A. Ensafi, H. Karimi-Maleh, *Int. J. Electrochem. Sci.* 5 (2010) 392.
28. A.J. Bard, L.R. Faulkner. Electrochemical Methods, Fundamentals and Application, 255, New York: Wiley, 2001.
29. Z. Galus, Fundumentals of Electrochemical Analysis, Ellis Horwood, New York. 1994.
30. J.N.Miller, J.C. Miller, Statistics and Chemometrics for Analytical Chemistry, 4th ed., Pearson Education Ltd., Edinburgh Gate, Harlow, Essex, England. 2000.